

Intelligent Sensorless Antilock Braking System for Brushless In-Wheel Electric Vehicles

Amir Dadashnialehi, *Member, IEEE*, Alireza Bab-Hadiashar, *Senior Member, IEEE*, Zhenwei Cao, and Ajay Kapoor

Abstract—Brushless motors are increasingly used in different designs of in-wheel electric vehicles (EVs). In this paper, a sensorless antilock braking system (ABS) for brushless-motor in-wheel EVs is proposed. The proposed solution omits the need for installation of separate conventional ABS sensors at each corner of the vehicle. This paper also shows, both theoretically and experimentally, that the general form of a conventional ABS sensor output voltage is identical to a brushless dc (BLDC)-motor back electromotive force. The proposed sensorless system can reduce the costs of manufacturing and maintenance of the vehicle and significantly improves the performance of the ABS by accurate wheel speed estimation and road identification using wavelet signal processing methods. The sensorless system was extensively tested using actual ABS hardware. Those experiments showed that the accuracy of the proposed sensorless wheel speed estimation for BLDC propulsion was higher than that of commercial ABS sensors. In addition, sensorless ABS for brushless propulsion was compared with that of brushed dc motor, and the results showed that the brushless sensorless ABS achieved better accuracy, robustness, and reliability compared with the sensorless ABS for brushed dc motor.

Index Terms—Antilock braking system (ABS), brushless motor, continuous wavelet transform (CWT), discrete wavelet transform (DWT), electric vehicle (EV), in-wheel technology, regenerative braking, sensorless ABS.

I. INTRODUCTION

THE antilock braking system (ABS) is a crucial safety system in modern vehicles. The role of the ABS is to maintain the steerability of the vehicle while trying to minimize the vehicle stopping distance in panic braking or challenging braking scenarios. In the last two decades, numerous attempts have been made to improve the performance of ABSs for conventional vehicles. As a result of using advanced control methods, the performance of ABS for conventional frictional brakes is close to optimal (see [1]–[6] and references therein). On the other hand, issues related to the design of ABSs for

electric vehicles (EVs) have recently gained attention [7], [8], and the problem of designing ABSs for in-wheel EVs is yet to be investigated.

In EVs that use the in-wheel design, a separate electric machine is available at each corner of the vehicle. These independent electrical machines provide unique opportunities for enhanced control strategies of the vehicle [9]. The availability of an electric machine at each corner of EV provides an additional degree of freedom in the design of the vehicle braking system as well. One approach is to use the regenerative back electromotive force (EMF) of the electric machine to recharge the EV batteries and produce regenerative braking torque to improve the performance of the braking system. However, in almost all existing EVs, it is common to disengage the regenerative braking torque during activation of ABSs and decelerate the vehicle entirely by the frictional braking torque [10]. The energy harvest during ABS activation cannot be economically justified as the ABS is rarely activated or is activated only for a very short time. The introduction of the additional regenerative braking torque could complicate the ABS control strategy and risks the safety of the vehicle. However, the regenerative back EMF of each in-wheel motor can still be effectively exploited to enhance the ABS of in-wheel EVs.

Recently, a sensorless ABS was introduced in [11], and simulation results in the paper showed that the back EMF of a *brushed* in-wheel EV can be used to estimate wheel speed and identify road condition in real time. An accurate wheel speed measurement system for sensorless ABS of a *brushed* in-wheel EV was realized in [12]. A more in-depth explanation of the above sensorless ABS was given in [13], which compared results of sensorless wheel speed estimations with measurement results of an actual ABS sensor. It was shown that the sensorless ABS introduced in [11]–[13] estimates the wheel speed with higher accuracy compared with ABS sensors and omits the need to install separate ABS sensors at each corner of the vehicle. The assumption underpinning this approach is that the regenerative back EMF can be used to simplify and improve the *wheel speed measurement* part of the ABS. This means that other parts of the ABS, including its controller, remain intact and the ABS standard or advanced control strategies that have been fully tested for many years and are legally approved can still be utilized.

The above sensorless ABS was solely considered for *brushed*-dc-motor-driven in-wheel EVs. A brushed permanent-magnet dc motor has a very simple dynamic: Its back-EMF analysis is straightforward, and its efficiency and maintenance requirement are suboptimal due to the use of brushes for commutation. On the other hand, in-wheel EVs require motors with

Manuscript received January 31, 2014; revised April 25, 2014; accepted June 7, 2014. Date of publication July 30, 2014; date of current version February 6, 2015. This work was supported by the Commonwealth of Australia through the Cooperative Research Centre for Advanced Automotive Technology Project C2-801, Electric Vehicle Control Systems and Power Management.

A. Dadashnialehi, Z. Cao, and A. Kapoor are with Swinburne University of Technology, Hawthorn, VIC 3122, Australia.

A. Bab-Hadiashar is with the School of Aerospace, Mechanical and Manufacturing Engineering, RMIT University, Melbourne, VIC 3122, Australia.

Color versions of one or more of the figures in this paper are available online at <http://ieeexplore.ieee.org>.

Digital Object Identifier 10.1109/TIE.2014.2341601

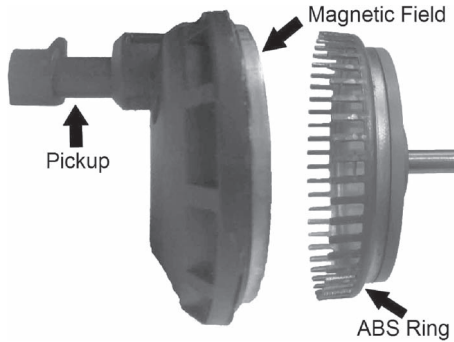


Fig. 1. Commercial ABS sensor (made by Repco Ltd.) used in sedan cars.

high efficiency and low maintenance for their propulsion system. As a result, brushless motors have gradually become the number one choice for almost all in-wheel EVs [8], [14]–[19]. This is despite the fact that the dynamics of brushless motors is more complicated than the brushed motors and therefore their back-EMF outputs are significantly different. In this paper, we investigate the feasibility of developing a sensorless ABS for brushless-motor-driven in-wheel EVs that would significantly reduce their maintenance and final cost and simplify their design. We will show that the back EMF of brushless motors, despite their complicated patterns, can be used to measure the wheel speed with similar (or better) accuracy compared with commercial ABS sensors and sensorless wheel speed measurement using brushed dc motors.

The rest of this paper is organized as follows. The existing wheel speed measurement technology for conventional ABS is described in Section II. The in-wheel design with brushless motor propulsion system is explained in Section III. The proposed intelligent sensorless ABS for brushless in-wheel hubs is introduced in Section IV. The fundamentals of the wavelet approach used for the analysis of the back-EMF signal are outlined in Section V. In Section VI, the experimental test rig and results of practical realization of the proposed sensorless ABS for brushless dc (BLDC) in-wheel hubs are presented and compared with a commercial ABS sensor and a sensorless ABS for brushed-dc-motor-driven in-wheel hubs. Section VII concludes this paper.

II. WHEEL SPEED MEASUREMENT IN ABS

The role of ABS sensor in ABSs is to measure the wheel rotational speed for the ABS controller. A typical commercial ABS sensor used in sedan cars is shown in Fig. 1. The ABS sensor is composed of a toothed ring (ABS ring), a permanent magnet, and a winding (pickup). The ABS ring is rotating with the vehicle wheel at the same rotational speed. The rotational motion of the ABS ring in the magnetic field of the permanent magnet induces a voltage in the winding. This voltage contains the wheel speed information and is used in conventional ABSs to estimate the wheel rotational speed.

The magnetic flux in the proximity of the ABS sensor winding can be modeled as follows:

$$\varphi_m = \varphi_0 \sin(n\theta) \quad (1)$$

where φ_0 is the constant flux produced by the permanent magnet of the ABS sensor, n is the number of teeth in the

ABS ring, and θ is the position of the ABS ring. According to Faraday's law, the EMF induced on the winding can be calculated as

$$\begin{aligned} V_{\text{ABS}} &= N \frac{d\varphi_m}{dt} \\ &= N\varphi_0 \frac{d(n\theta)}{dt} \cos(n\theta) \\ &= N\varphi_0 n\omega \cos(n\theta) \end{aligned} \quad (2)$$

where N is the number of coils in the winding and is the angular velocity of the ABS ring. Although (2) shows that both amplitude and frequency of the ABS sensor output voltage are directly proportional to the rotational speed of the ABS ring, the frequency information is commonly used for wheel speed measurement. As such, for comparison purposes, we have also used the *frequency method* in our experiments to calculate the wheel speed from the ABS sensor output.

We will show (theoretically in Section III and experimentally in Section IV) that the general form of a conventional ABS sensor output voltage, modeled by (2), is identical to BLDC-motor back EMF. This is an important step in making the ABS sensor redundant for the design of sensorless ABS for brushless in-wheel EVs.

III. IN-WHEEL DESIGN WITH BRUSHLESS PROPULSION

In-wheel EVs are designed based on the idea of transferring the propulsion system of the vehicle to its wheels. An assembly that includes a separate electric motor as its propulsion system, as well as other important components such as a frictional brake and a suspension spring, is called an in-wheel hub. Electric motors of the in-wheel hubs are desired to have high efficiency, small size, and low maintenance requirements. Permanent-magnet brushless (PMBL) motors possess these characteristics and are predominantly employed in in-wheel hubs.

Permanent-magnet synchronous motors (PMSMs) and BLDC motors are two types of PMBL machines that have the same construction. The required magnetic fields of both machines are generated by the rotors having permanent magnets, and their armature windings, which are connected to three-phase voltage sources, are located on their stators [20]. The PMSM is fed by a three-phase sinusoidal voltage, whereas the BLDC motor is connected to a dc-chopped three-phase voltage source. Although the back-EMF shapes in PMSMs and BLDC motors are different when those are driven, the back EMF of both machines as generators are sinusoidal shape voltages. In this paper, we use the back EMF of the brushless machine in the generator mode, and the focus is on the BLDC machine back EMF in the regenerative mode of operation henceforth.

A BLDC motor consists of a PMSM, a position sensor (Hall-effect sensors), and an inverter that electronically implements the commutation for the motor [21]. An electronically commutated BLDC motor is shown in Fig. 2.

The equivalent circuit of phase A of the BLDC machine (see Fig. 2) is shown in Fig. 3. Base on this model, the voltage of phase A can be expressed as

$$V_A = R_A I_A + L_A \frac{dI_A}{dt} + e_A \quad (3)$$

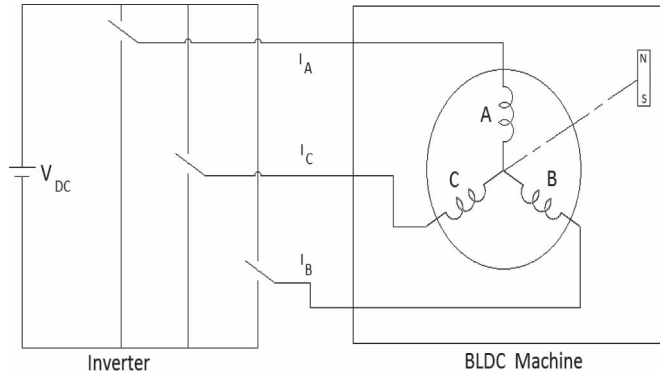


Fig. 2. Electronically commutated BLDC motor.

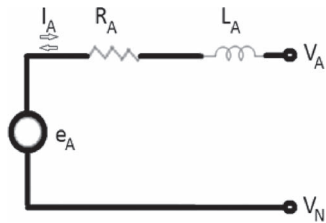


Fig. 3. Equivalent circuit of BLDC machine (phase A).

where R_A and L_A are the equivalent resistance and inductance of the stator phase winding, I_A is the current flowing in phase A, and e_A is the back EMF of this phase.

The back-EMF voltage of the phase A of a BLDC machine can be expressed as

$$e_A = K\omega_e \cos \theta_e \quad (4)$$

where ω_e and θ_e are the electrical velocity and position of the rotor, and K is a constant. Equation (4) shows that the amplitude of the back EMF increases as the speed increases. This is similar to the relationship between the amplitude of the ABS sensor output and the wheel rotational speed. The rotor electrical position (θ_e) is related to the mechanical position (θ_m) by

$$\theta_e = N_p \theta_m \quad (5)$$

where N_p is the number of pole pairs of the rotor. Equations (4) and (5) show that the back-EMF signal completes N_p cycles per each complete rotation of the BLDC rotor. This is similar to the relationship between voltage and frequency of the ABS sensor signal shown in (2).

In the succeeding section, we introduce an intelligent sensorless ABS that exploits the information contained in the BLDC-back-EMF signal to eliminate the need to install separate ABS sensors in BLDC driven in-wheel EVs.

IV. INTELLIGENT SENSORLESS ABS

The term “sensorless” in BLDC-motor control literature is often used to denote the motor position/speed control methods that do not require a separate position/speed sensor. A technical review of position and speed sensorless control methods of

BLDC motors is given in [22]. Sensorless control techniques have also been applied to brushless-motor-driven EVs. For example, a hybrid sliding-mode control method of BLDC-motor-driven EVs was proposed in [15]. Despite the fact that the motivations behind both sensorless control and sensorless wheel speed measurement for ABS are similar (i.e., to eliminate the need for position/speed sensors), their operations are very different. The BLDC-motor sensorless control methods exploit the back EMF to estimate “current commutation points” in motor operation mode. The sensorless ABS is however intended to provide continuous wheel speed estimation during ABS activation when the BLDC is operating as a generator.

The idea of eliminating the ABS sensor stems from the fact that ABS sensors used in conventional ABSs have several disadvantages. The ABS ring, which is the most important component of the ABS sensor, is relatively bulky and makes dimensions of the sensor larger than typical sensors. As it was mentioned earlier, several components (such as propulsion, suspension, and braking systems) should be integrated inside a limited space of the in-wheel hub. As such, omitting the ABS sensor saves critical space for a better in-wheel design. The ABS ring is also vulnerable to dust and corrosion, as well as wheel hub inspection or repair procedures. The ABS sensor output is sensitive to the gap space between the ABS rings and the permanent magnet of the sensor. This space is hard to adjust, and a slight misalignment of this space influences the sensor’s output. Additional wiring is also required for transmitting the output signal to the ABS controller. This signal can also be influenced by external disturbances. In contrast to conventional vehicles, for which the current generation of ABS sensors is designed, the existence of a powerful electric motor in hubs of EVs means that a significant source of disturbance, which can distort the ABS signal and deteriorate its performance, is unavoidable. ABS speed measurements are also susceptible to mechanical faults in the wheel bearing assembly and electrical faults such as occurrences of open/short circuit and change of wire resistance [13].

The sensorless ABS design for in-wheel EVs is one way to address the above issues. It should also be noted that the assembly, inspection, and maintenance of in-wheel hubs are more complex and time-consuming compared with traditional wheel hubs. The sensorless ABS simplifies the inspection and maintenance procedures of the in-wheel EVs and reduces the final price and on-going maintenance costs of the vehicle [13].

An important step in making the ABS sensor redundant is to find a way to estimate the wheel speed from other available signals in the in-wheel hub. We earlier argued that the output voltage of the ABS sensor is similar to the back-EMF voltage of the brushless generators. In addition, the regenerative braking torque is commonly disengaged during activation of ABS [10]. This means that, during the activation of ABS, all phases (including phase A of the BLDC machine shown in Fig. 2) are open circuited and the current in each phase is zero (e.g., $I_A = 0$ in phase A). As such, (3) for ABS activation can be simplified to

$$V_A = e_A. \quad (6)$$

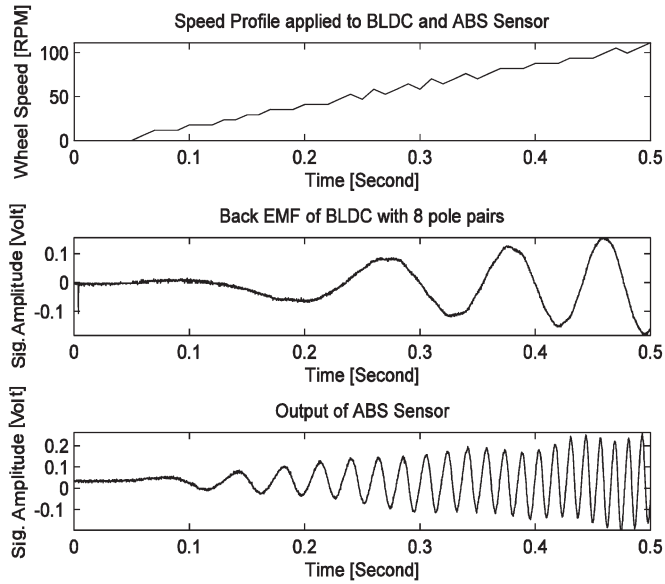


Fig. 4. Comparison between a 48-tooth ABS sensor (made by Repco Ltd.) output and BLDC motor (with eight-pole pair) back EMF.

Equation (6) shows that the voltage of phase A is equal to the BLDC back EMF and it would be possible to use the voltage of phase A to estimate the wheel speed.

To show the similarity of the BLDC back-EMF and ABS sensor signals, we conducted an experiment in which the ABS ring of a commercial ABS sensor was connected to the rotor of a BLDC motor. The output of the ABS sensor and the back EMF of the connected BLDC machine were recorded and compared. An output voltage of a commercial ABS sensor (with 48 teeth) while it is connected to the rotor of a BLDC motor (with eight pole pairs) is shown in Fig. 4. The figure shows that the magnitude and the frequency of both signals would generally increase as the wheel speed increases.

We showed earlier section that both the magnitude and the frequency of output voltages of the ABS sensor and the BLDC machine are directly proportional to the wheel speed. It was also mentioned that wheel speed measurement from the output of the ABS sensor is currently based on calculation of the frequency of this signal (the *frequency method*). The measurement resolution of ABS sensor is related to the number of teeth in the ABS ring (typically 48 teeth). Although the same frequency method can also be applied to the BLDC back-EMF voltage to measure the wheel speed during ABS activation, the BLDC machine integrated in the in-wheel hub must have enough pole pairs (at least 24 pole pairs) to provide the same measurement accuracy and resolution compared with the ABS sensor.

To overcome the above restriction, we propose to use the amplitude of the BLDC-back-EMF signal and developed an algorithm (see Section VI for details) that uses this source of information to estimate the wheel speed during ABS activation. Our experiments (see Section VI) also confirmed that wheel speed estimation by using the amplitude method can alleviate the constraint on the number of pole pairs down to only two pole pairs, where the wheel speed measurement accuracy is almost comparable to ABS sensor measurements. We also show that the accuracy of the amplitude method significantly increases

for BLDC machines with more than two pole pairs (which is not possible using the standard frequency method for BLDC motors).

A review of the research literature of the last decade suggests that, in practice, it is both common and important to devise additional signal processing algorithms to compensate for the deteriorating effect of noise on the ABS sensor accuracy. For instance, the importance of accurate wheel speed estimation in the ABS was investigated in [13] and [23]. The authors studied the performance of a practical bang-bang (on/off) ABS controller in the presence of noisy wheel speed measurements. Their analysis showed that the stopping distance of the vehicle significantly increases as the power of noise on the wheel speed estimation increases. As such, it is important to increase the accuracy of wheel speed estimation for optimum performance of the ABS. Moreover, several attempts have been made to improve the existing wheel-speed-sensor measurements using advanced signal processing methods. In [24], an adaptive line enhancer (ALE) based on an adaptive algorithm was used to improve the response of a wheel speed sensor. A frequency-domain least-mean-square adaptive filter was also used to cancel noise in a wheel speed sensor, and the experiment results showed that it is important to use digital signal processing methods in the presence of noise [25]. In [26], a prediction algorithm based on a second-order polynomial curve fitting algorithm was proposed to estimate the wheel speed signal.

Although our experimental results showed that the amplitude method was able to estimate the wheel speed with accuracy rates comparable to the ABS sensor measurement, the required accuracy for a low number of pole pairs (two pole pairs) could not have been guaranteed. To ensure the attainment of required accuracy, an intelligent sensorless ABS using the wavelet signal processing method is also developed. The word intelligent here signifies the fact that the proposed system would improve the ABS performance by both increasing the wheel speed measurement accuracy and conducting road identification to keep the ABS in its stable region. Road identification is an important and challenging issue for optimum performance of ABSs (see [11], [13] and references therein). The braking process on roads with different surface conditions (such as dry or icy) results in different features in the BLDC-back-EMF signal of the in-wheel hub. These features can be extracted by CWT of the back-EMF signal during ABS activation for road identification purposes.

A. Robustness and Reliability

An important advantage of using BLDC motors stems from the fact that the availability of three separate back-EMF signals can be exploited to improve the robustness and reliability of the proposed sensorless ABS. It should be noted that this opportunity is not available for brushed-motor in-wheel EVs because brushed dc motors have only one phase.

Since ABS sensors in a vehicle use separate windings and wirings for transmission of their output signals to the ABS controllers, their output voltages are susceptible to system faults and disturbances. A common fault in ABS sensors is the short circuit fault by which the wheel speed feedback is completely lost. As a result, the ABS control system will be forced to

operate in an open-loop mode, and the vehicle's ABS would be deactivated as there is no alternative source of information to provide redundancy.

On the contrary, the speed information for the sensorless ABS for BLDC-motor in-wheel EV is readily available in each of the three separate phases of the BLDC machine. This means that the information carried by each phase can be used as a separate ABS sensor measurement. This redundancy can be effectively used to improve the robustness and reliability of the sensorless ABS for in-wheel EVs. Simple aggregation operators such as mean or median can be easily implemented in the measurement system of the sensorless ABS to address the robustness and reliability issues.

If a conventional ABS sensor was short-circuited, there would be no substitute source of speed information and ABS would not work. However, even if one phase of BLDC is short-circuited, the implementation of a simple aggregation operator can still provide speed measurement. To study this situation, we conducted several experiments and tested the performance of simple aggregation operators. The results of these experiments are outlined in Section VI.

V. BACK-EMF ANALYSIS BY WAVELETS

To attain the required ABS performance mentioned earlier, we propose to use back-EMF processing techniques based on discrete and CWTs. We show that these techniques provide the required wheel speed estimation accuracy and road identification ability.

A. Accurate Wheel Speed Estimation Using DWT

The discrete wavelet transform (DWT) of a discrete signal is given by

$$\text{DWT}[j, k] = \sum_n x[n]h_j^*[n - 2^j k] \quad (7)$$

where n represent sample points of the signal, and j and k ($j \in \mathbb{N}, k \in \mathbb{Z}$) are scale and shift parameters, respectively. DWT uses a dyadic time–frequency decomposition structure that provides low- and high-frequency components of a given signal at each decomposition level. The low- and high-frequency components are referred to as approximations A_i and details D_i at level i , respectively (see Fig. 5). While approximations of a given signal represent the smooth variations, the details are related to abrupt changes in the signal.

The proposed amplitude method in Section IV is able to provide wheel speed estimation using the BLDC back EMF during ABS activation. However, the wheel speed accuracy obtained by using this method deteriorates for BLDC motors with a very low number of pole pairs (e.g., two pole pairs). Our experiments, detailed in Section VI, showed that the wheel speed signal (achieved by the amplitude method) for a BLDC with two pole pairs has a higher frequency content compared with its counterpart signal for a BLDC motor with eight pole pairs. This high frequency content contains abrupt changes that degrade the accuracy of wheel speed estimations for BLDC motors with a low number of pole pairs.

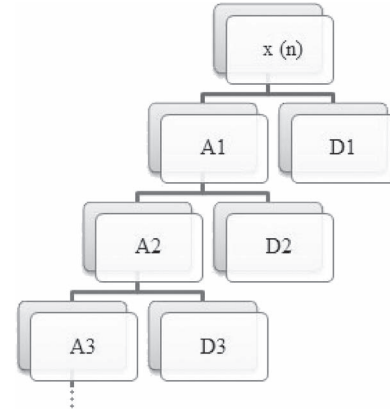


Fig. 5. Implementation structure of DWT.

To improve the accuracy of wheel speed estimations for BLDC motors with a low number of pole pairs, we propose to decompose the wheel speed signal achieved by the amplitude method by using the DWT decomposition with a structure that is shown in Fig. 5. The proposed technique based on DWT identifies the low-frequency component (approximations) that contains accurate wheel speed estimations. In our experiments, shown in Section VI, we observed that the wheel speed estimation error significantly decreases by using the approximations of the inaccurate wheel speed estimation (by the amplitude method) at level 7 A_7 , for a BLDC motor with a low number of (only two) pole pairs.

B. Road Identification Using CWT

The CWT of signal $x(t)$ is given by

$$\text{CWT}(a, b) = \frac{1}{\sqrt{a}} \int_{-\infty}^{+\infty} x(t)\psi^*\left(\frac{t-a}{b}\right) dt \quad (8)$$

where $\psi^*(t)$ is a complex conjugate of a wavelet function, and a and b are scale and shift values, respectively. Unlike DWT, the scale and shift parameters in the CWT are real values. This enables an effective time–frequency representation of a signal that can be used for local feature extraction.

The implementation detail of our proposed CWT-based feature extraction algorithm for road identification is as follows. The first step is to compute the CWT of the BLDC-back-EMF signal using the *Morlet wavelet*. We then define and use the following energy index to distinguish between different road conditions:

$$\text{Energy_Index}(n) = \sqrt{\sum_{i=1}^n \sum_{s=2}^{20} \text{Coef}_i(s)^2} \quad (9)$$

where n represent the sample points of the BLDC-back-EMF signal and s , and Coef_i are CWT scales and coefficients, respectively. Our experiments, presented in Section VI, showed that the road condition features can be extracted by calculating the above energy index for BLDC back EMF. Our experiments also showed that the above energy index for road identification is an appropriate measure for road identification purposes

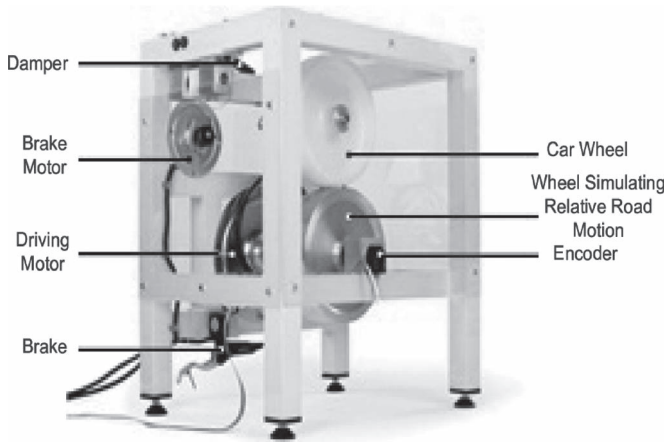


Fig. 6. Standard ABS setup (made by Inteco) for frictional brakes [27].

because its values are significantly higher for slippery roads (e.g., icy or oily roads) compared with roads with higher friction coefficients (e.g., dry asphalt). For this reason, we use the above energy index for road identification during ABS activation.

VI. EXPERIMENTAL RESULTS AND DISCUSSION

A. Experimental Setup

To investigate the feasibility of developing sensorless ABS for brushless in-wheel EVs, we modified a commonly used experimental ABS test rig [27], which is shown in Fig. 6, to include different BLDC motors (with a different number of pole pairs) representing the propulsion system of the vehicle. The standard test rig is originally designed to test the performance of ABS for frictional brakes and includes two wheels that simulate the car wheel motion and the relative motion of the vehicle by the upper and lower wheels, respectively.

A typical experiment with the ABS test rig starts by bringing both the upper and lower wheels to a predefined initial speed, which is the vehicle wheel speed at the start of the braking phase. For this purpose, a driving motor is coupled to the lower wheel to achieve the desired velocity. When the speed of the upper wheel (car wheel) reaches a predefined value (initial speed of the braking phase), the driving motor is switched off, and the braking phase starts. The braking mechanism in this test rig is based on using a disk brake, which is mounted on the upper wheel. The ABS of this test rig uses the on/off (bang-bang) controller to avoid locking of the upper wheel. Rotational velocities of both wheels are measured by using two highly accurate optical encoders.

In addition to modifying the above standard ABS test rig to include two different BLDC motors (with two and eight pole pairs), a commercial ABS sensor (used in many sedan vehicles, made by Repco) was also coupled to the upper wheel to compare the result of sensorless wheel speed measurement with a commonly used commercial ABS sensor (see Fig. 7).

Sensorless wheel speed estimation of dc-motor-driven in-wheel EVs was studied in [13]. To compare the results of BLDC with dc-motor speed estimation during activation of ABS, a dc motor was also connected to the upper wheel shaft. With the above modifications, wheel speed can be estimated

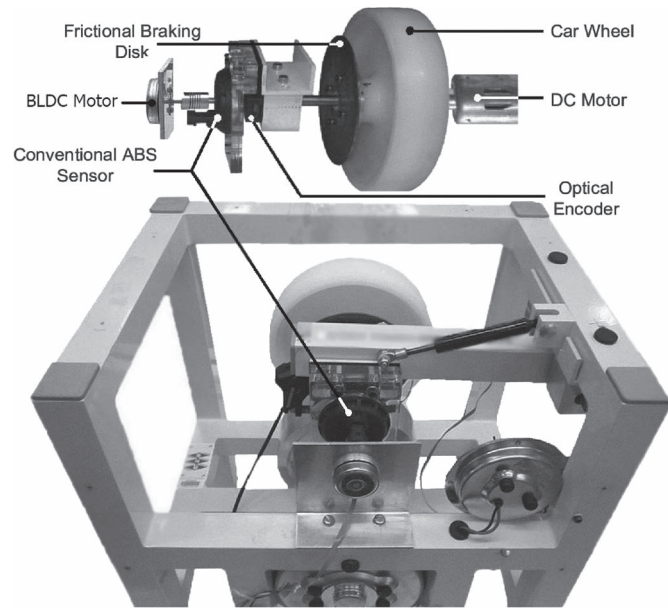


Fig. 7. Installation details of the modified ABS test rig for realizing the sensorless ABS.

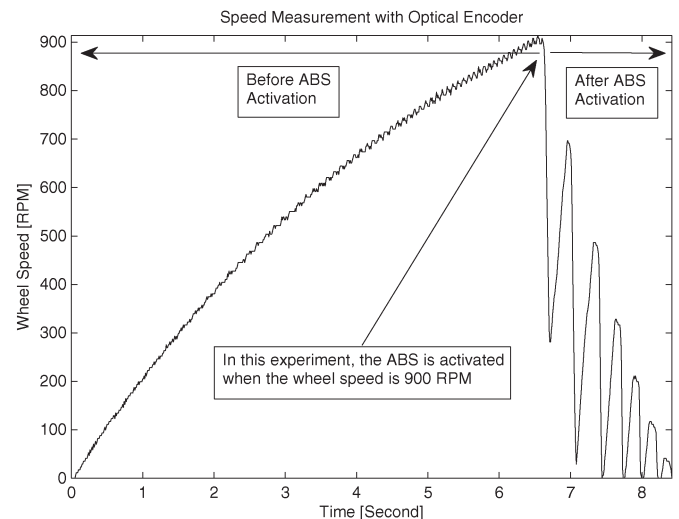


Fig. 8. Typical reference wheel speed measurements by optical encoder during a complete experiment.

and compared using four different methods: BLDC sensorless ABS, permanent-magnet dc sensorless ABS, commercial ABS sensor, and the test rig optical encoders (as the reference measurements). The juxtaposition of the added hardware on the test rig is shown in Fig. 7.

B. Results and Discussion

The reference wheel speed provided by the optical encoder before and after ABS activation in an experiment where the ABS is activated at around 900 RPM, and its corresponding ABS sensor output are shown in Figs. 8 and 9. The wheel speed measurements (during ABS activation) from the ABS sensor output (using the standard frequency method [13]) is depicted in Fig. 10. We will refer to the above wheel speed measurements as ABS sensor measurements henceforth.

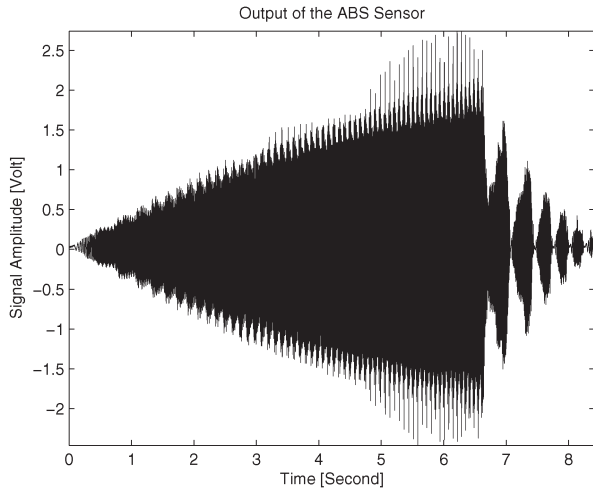


Fig. 9. Unprocessed output of ABS sensor corresponding to Fig. 8.

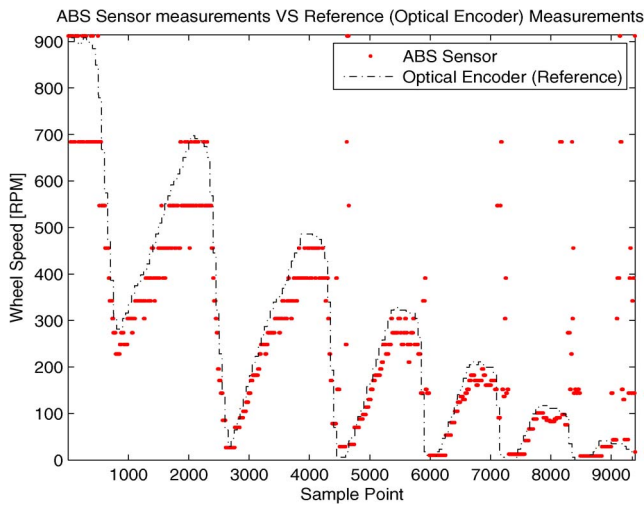


Fig. 10. Comparison between ABS sensor measurements and reference (optical encoder) measurements during ABS activation.

To compare the accuracy of different wheel speed measurement methods, we calculated the mean absolute error (MAE) and the RMSE indexes for measurement results of those techniques. Mean absolute error (MAE) is defined as

$$\text{MAE} = \frac{\sum_{i=1}^n |\text{Sig}(i) - \text{Ref}(i)|}{n} \quad (10)$$

where n is the number of sample points and $\text{Sig}(i)$ and $\text{Ref}(i)$ denote the measured values for the i th sample point provided by the chosen technique and reference measurement. The other error index, i.e., RMSE, which emphasizes the importance of larger errors, is defined in (11). The MAE and RMSE values for ABS measurements during ABS activation are calculated to be 70.6 and 127.2, respectively,

$$\text{RMSE} = \sqrt{\frac{\sum_{i=1}^n (\text{Sig}(i) - \text{Ref}(i))^2}{n}} \quad (11)$$

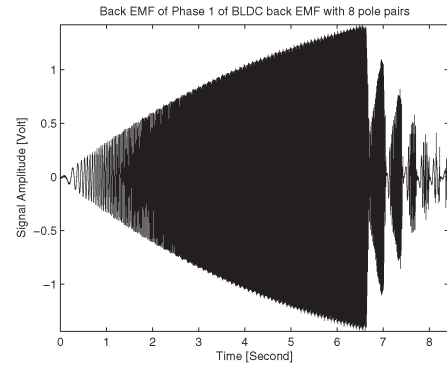


Fig. 11. BLDC Back EMF (with eight pole pairs) corresponding to Fig. 8.

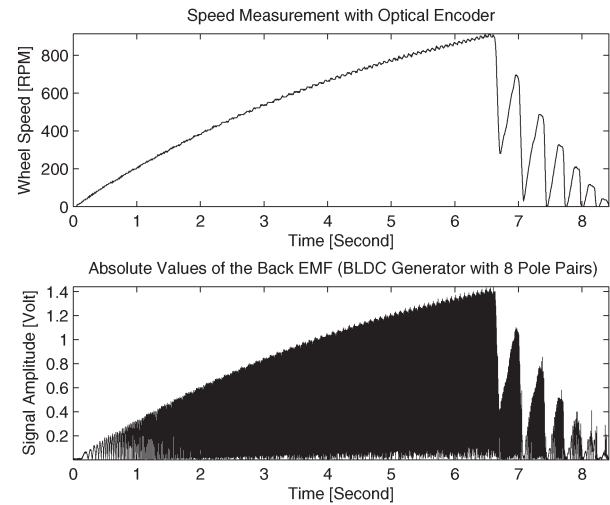


Fig. 12. Top: Reference (optical encoder) measurements. Bottom: Absolute values of the back-EMF signal shown in Fig. 11.

1) Amplitude Method: The back EMF of a BLDC machine (with *eight pole pairs*) corresponding to Fig. 8 is shown in Fig. 11. In order to show that the wheel speed can be estimated from the amplitude of the BLDC back EMF, the absolute values of the amplitudes of the back-EMF signal shown in Fig. 11 are likewise plotted in Fig. 12. This figure shows that there is a high correlation between the absolute values of the BLDC-back-EMF signal and reference measurements. The signal shown in the bottom part of Fig. 12 (which is referred to as the amplitude signal hereafter) has a higher frequency content compared with the reference signal (top part of Fig. 12). We propose to use local maxima of the amplitude signal to generate a smoother signal with a lower frequency content (similar to the reference wheel speed signal). A local maximum is defined as a data sample of the amplitude signal that is larger than its neighboring values (immediate neighbors). The combination of peak detection (that identifies those local maximums) and extrapolation algorithms was then used to reconstruct the wheel speed signal. Result of applying the peak detection and extrapolation algorithms on the amplitude signal shown in Fig. 12 is shown in Fig. 13 (which is referred to as the “peak signal” hereafter).

The MAE and RMSE values for the wheel speed estimation using the amplitude method (see Fig. 13) are 29.5 and 57.5, respectively. These results show that the MAE and RMSE of the amplitude method are 58.2% and 54.8% lower than their

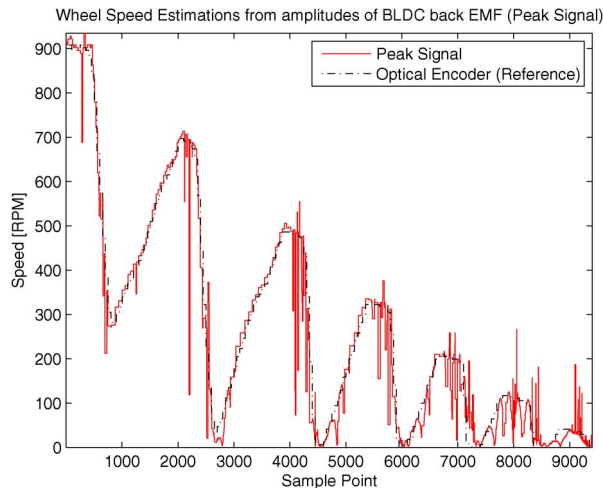


Fig. 13. Peak signal (wheel speed estimations using the amplitude method) corresponding to the amplitude signal shown in Fig. 12.

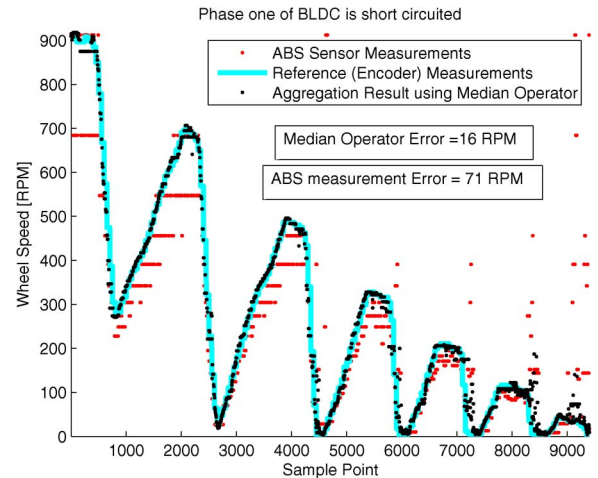


Fig. 15. Result of aggregating wheel speed measurements (using the amplitude method) by median operator.

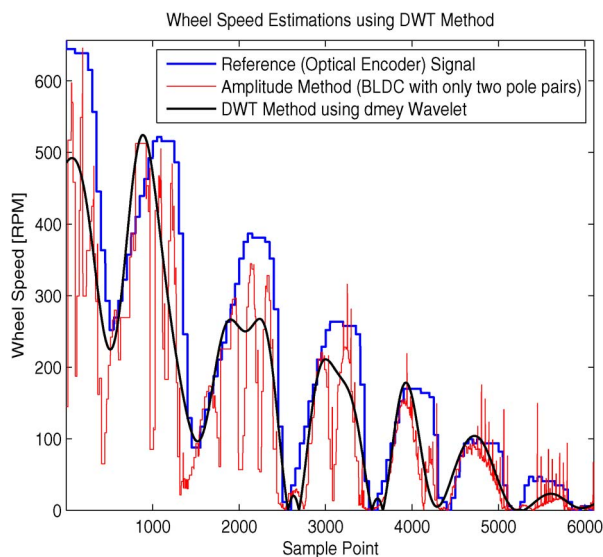


Fig. 14. Wheel speed estimation from EMF of a BLDC with only two pole pairs using the DWT method.

corresponding values for the ABS sensor measurements. The results of calculating the MAE and RMSE values for numerous experiments (with different road conditions and initial speeds for the start of the braking phase) showed that the accuracy of wheel speed estimation using the amplitude method are always significantly higher than the accuracy of ABS sensor measurements. It should however be noted that the full validation of the proposed sensorless ABS for a particular type of a vehicle requires extensive testing on that particular model.

2) DWT Method: To ensure that better wheel speed estimation accuracy, compared with those produced by the commercial ABS sensor, is always achieved (particularly, for BLDC motors with a low number of pole pairs), a more sophisticated method based on using DWT (the DWT method described in Section V) was used. Fig. 14 shows that the DWT method successfully extracts the underlying smooth wheel speed signal from the speed measurements by the amplitude method for a BLDC with only two pole pairs.

It is important to choose a suitable wavelet shape in this method. To this end, we investigated different wavelet shapes (Haar, db2-db10, sym2-sym8, coif1-5, bior1.1-bior6.8, rbio1.1-rbio6.8, and dmey wavelets), and the dmey wavelet extracted the most similar underlying wheel speed signal, as shown in Fig. 14. The results of calculating MAE and RMSE values for the wheel speed estimation (see Fig. 14) by using the DWT method showed that the method's accuracy is significantly higher compared with that of ABS sensor (MAE and RMSE values decrease 34% and 48%, respectively).

3) Robustness and Reliability: To study the robustness and reliability of the proposed sensorless system, we conducted a few experiments by assuming that a phase of the BLDC motor is short-circuited while a simple (e.g., median) aggregation operator is implemented. Experimental results showed that accuracy of the aggregated results using the median operator is still higher than the accuracy of ABS sensor measurements even when there is a fault.

Fig. 15 shows the result of aggregating wheel speed measurements (using the amplitude method) by median operator, where phase one of the BLDC is short-circuited. The figure shows that the (mean of) error for the aggregated result (16 r/min) is 77% less than that of ABS sensor measurements (71 RPM), despite the fact that phase one of the BLDC is short-circuited.

4) Comparison Between Sensorless Wheel Speed Estimation for BLDC and DC Motors: Wheel speed estimation from dc-motor back EMF corresponding to Fig. 10 are shown in Fig. 16. The RMSE values were approximately the same for both brushed and brushless motors. However, the MAE value for brushed dc motor was calculated to be 7% higher compared with that of BLDC-motor back-EMF speed measurement, which shows that wheel speed estimation for the BLDC with eight pole pairs (using the amplitude method) is more accurate compared with the dc-motor back-EMF wheel speed measurement.

As it was shown in [13], the back EMF in the dc motor is linearly related to its armature speed, and this relationship simplifies sensorless wheel speed estimation for ABS for dc-driven in-wheel EVs. In practice, however, the back-EMF noise, which

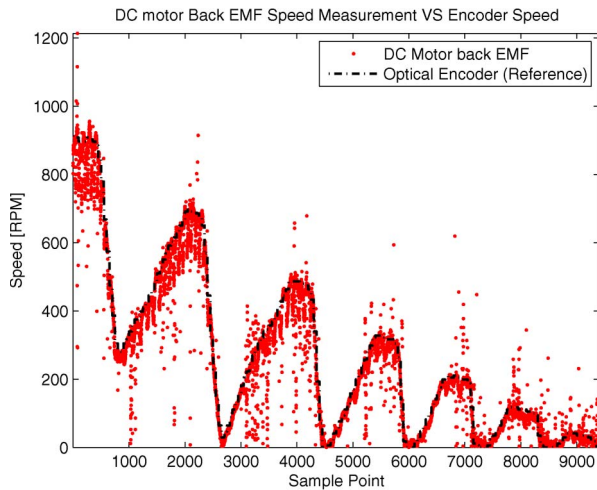


Fig. 16. DC-motor back-EMF speed measurement.

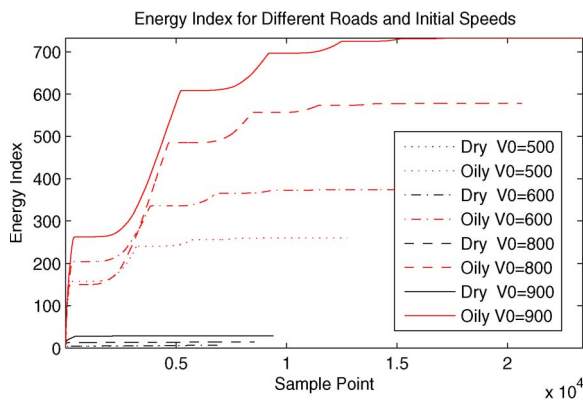


Fig. 17. Energy index for different road conditions and initial speeds.

is produced by brushes in the dc machine, degrades the wheel speed estimation accuracy. On the contrary, the BLDC motor does not have mechanical brushes, and as such, BLDC back EMF is less noisy compared with that of the dc motor. For this reason, the proposed amplitude method for sensorless wheel speed estimation of BLDC motors was expected to produce better accuracy compared with dc motors.

5) Road Identification Using the CWT Method: To validate the proposed road identification method, outlined in Section V, we carried out several experiments with two different road conditions (slippery road and dry road) to produce real BLDC-back-EMF signals during ABS activation. We covered road surface with oil in our experiments to create slippery road condition. The back-EMF signals (related to dry and slippery road condition) were captured and analyzed with different continuous wavelets. The wavelet shape is important in road identification using (9), and our experiments showed that the Morlet wavelet is the most suitable wavelet for this purpose. Fig. 17 shows the calculated energy index [defined in (9)] in different experiments (with different road conditions and different initial speed for the start of the braking phase), using the Morlet wavelet. The results show that the proposed energy index is sensitive to road conditions as its value significantly increases for slippery road compared with dry road and can be used for road identification purposes.

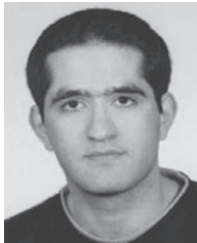
VII. CONCLUSION

Brushless motors are currently the dominant choice for the propulsion system of in-wheel EVs. We showed that the back-EMF signal of brushless in-wheel hubs can be exploited to simplify their ABS arrangement. The proposed innovative design reduces the final and ongoing maintenance costs of the vehicle by eliminating the need to install separate ABS sensors. Our experiments showed that the proposed intelligent sensorless ABS is able to produce accurate wheel speed estimation and perform road identification, which both significantly contribute to the ABS performance. We conducted a number of experiments with different road conditions and showed that the accuracy of the proposed method is higher than that of commercial ABS sensors; hence, the need for a separate sensor can be eliminated. Specifically, experimental results show that the sensorless wheel speed measurement accuracy of a BLDC motor with eight pole pairs is approximately 50% better than the ones produced by the commercial ABS sensor. Those results also show that the measurement accuracy for motors with a very low number of pole pairs (e.g., only two pole pairs) is still approximately 40% better than the commercial sensors when the DWT method is applied. The robustness of the sensorless ABS for BLDC was also compared with that of conventional ABS, and the results showed that the robustness was significantly improved by implementing simple aggregation operators on wheel speed information obtained from three phases of BLDC.

REFERENCES

- [1] Y. Oniz, E. Kayacan, and O. Kaynak, "A dynamic method to forecast the wheel slip for antilock braking system and its experimental evaluation," *IEEE Trans. Syst., Man, Cybern. B, Cybern.*, vol. 39, no. 2, pp. 551–560, Apr. 2009.
- [2] W. Y. Wang, I. H. Li, M. C. Chen, S. F. Su, and S. B. Hsu, "Dynamic slip-ratio estimation and control of antilock braking systems using an observer-based direct adaptive fuzzy-neural controller," *IEEE Trans. Ind. Electron.*, vol. 56, no. 5, pp. 1746–1756, May 2009.
- [3] R. Hoseinnezhad and A. Bab-Hadiashar, "Efficient antilock braking by direct maximization of tire-road frictions," *IEEE Trans. Ind. Electron.*, vol. 58, no. 8, pp. 3593–3600, Aug. 2011.
- [4] N. Mutoh, Y. Hayano, H. Yahagi, and K. Takita, "Electric braking control methods for electric vehicles with independently driven front and rear wheels," *IEEE Trans. Ind. Electron.*, vol. 54, no. 2, pp. 1168–1176, Apr. 2007.
- [5] E. Kayacan, Y. Oniz, and O. Kaynak, "A grey system modeling approach for sliding-mode control of antilock braking system," *IEEE Trans. Ind. Electron.*, vol. 56, no. 8, pp. 3244–3252, Aug. 2009.
- [6] A. V. Topalov, Y. Oniz, E. Kayacan, and O. Kaynak, "Neuro-fuzzy control of antilock braking system using sliding mode incremental learning algorithm," *Neurocomputing*, vol. 74, no. 11, pp. 1883–1893, May 2011.
- [7] R. de Castro, R. E. Araujo, and D. Freitas, "Wheel slip control of EVs based on sliding mode technique with conditional integrators," *IEEE Trans. Ind. Electron.*, vol. 60, no. 8, pp. 3256–3271, Aug. 2013.
- [8] L. Weng-Ching, L. Chun-Liang, H. Ping-Min, and W. Meng-Tzong, "Realization of anti-lock braking strategy for electric scooters," *IEEE Trans. Ind. Electron.*, vol. 61, no. 6, pp. 2826–2833, Jun. 2014.
- [9] Y. Hori, "Future vehicle driven by electricity and control—Research on four-wheel-motored 'UOT Electric March II,'" *IEEE Trans. Ind. Electron.*, vol. 51, no. 5, pp. 954–962, Oct. 2004.
- [10] R. C. Kosik, S. O. Pate, and W. F. Sanderson, "Temperature compensated lift-throttle regenerative braking," U.S. Patent 6588860B2, Jul. 8, 2003.
- [11] A. Dadashnialehi, Z. Cao, A. Kapoor, and A. Bab-Hadiashar, "Intelligent sensorless ABS for regenerative brakes," in *Proc. IEEE IEVC*, 2012, pp. 1–5.
- [12] A. Dadashnialehi, A. Bab-Hadiashar, Z. Cao, and A. Kapoor, "Accurate wheel speed measurement for sensorless ABS in electric vehicle," in *Proc. IEEE ICVES*, 2012, pp. 37–42.

- [13] A. Dadashnialehi, A. Bab-Hadiashar, Z. Cao, and A. Kapoor, "Intelligent sensorless ABS for in-wheel electric vehicles," *IEEE Trans. Ind. Electron.*, vol. 61, no. 4, pp. 1957–1969, Apr. 2014.
- [14] M. Terashima *et al.*, "Novel motors and controllers for high-performance electric vehicle with four in-wheel motors," *IEEE Trans. Ind. Electron.*, vol. 44, no. 1, pp. 28–38, Feb. 1997.
- [15] Y. Wang, X. Zhang, X. Yuan, and G. Liu, "Position-sensorless hybrid sliding-mode control of electric vehicles with brushless DC motor," *IEEE Trans. Veh. Technol.*, vol. 60, no. 2, pp. 421–432, Feb. 2011.
- [16] H. Kahveci, H. I. Okumus, and M. Ekici, "An electronic differential system using fuzzy logic speed controlled in-wheel brushless DC motors," in *Proc. Powereng*, 2013, pp. 881–885.
- [17] R. Vandana and B. G. Fernandes, "Optimal sizing of motor—Battery system for in wheel electric vehicles," in *Proc. IEEE IECON*, pp. 2510–2515.
- [18] M. G. Simoes and P. Vieira, Jr., "A high-torque low-speed multiphase brushless machine—a perspective application for electric vehicles," *IEEE Trans. Ind. Electron.*, vol. 49, no. 5, pp. 1154–1164, Oct. 2002.
- [19] K. T. Chau, C. C. Chan, and L. Chunhua, "Overview of permanent-magnet brushless drives for electric and hybrid electric vehicles," *IEEE Trans. Ind. Electron.*, vol. 55, no. 6, pp. 2246–2257, Jun. 2008.
- [20] X. Zhang and C. Mi, *Vehicle Power Management Modeling, Control and Optimization*. New York, NY, USA: Springer-Verlag, 2011.
- [21] S. Ogasawara and H. Akagi, "An approach to position sensorless drive for brushless DC motors," *IEEE Trans. Ind. Appl.*, vol. 27, no. 5, pp. 928–933, Sep./Oct. 1991.
- [22] P. P. Acarnley and J. F. Watson, "Review of position-sensorless operation of brushless permanent-magnet machines," *IEEE Trans. Ind. Electron.*, vol. 53, no. 2, pp. 352–362, Apr. 2006.
- [23] A. Dadashnialehi, A. Bab-Hadiashar, Z. Cao, and A. Kapoor, "Enhanced ABS for in-wheel electric vehicles using data fusion," in *Proc. IEEE IV Gold Coast*, Australia, 2013, pp. 702–707.
- [24] W. Hernández, "Improving the response of a wheel speed sensor using an adaptive line enhancer," *Measurement*, vol. 33, no. 3, pp. 229–240, Apr. 2003.
- [25] W. Hernández, "Improving the response of a wheel speed sensor by using frequency-domain adaptive filtering," *IEEE Sensors J.*, vol. 3, no. 4, pp. 404–413, Aug. 2003.
- [26] G. Liu, Q. Zhang, Y. Wang, Z. Dong, and B. Liu, "Analysis of the ABS wheel speed signal error and method of equal period sampling," in *Proc. Int. Conf. Inf. Acquisition*, Aug. 20–23, 2006, pp. 994–999.
- [27] *The Laboratory Antilock Braking System Controlled from PC*, Inteco Ltd., Krakow, Poland, 2011.



Amir Dadashnialehi (M'14) was born in Iran in 1982. He received the B.Sc. and M.Sc. degrees in electrical engineering from the University of Tehran, Tehran, Iran, in 2005 and 2008, respectively. He is currently working toward the Ph.D. degree in the Faculty of Engineering and Industrial Sciences, Swinburne University of Technology, Hawthorn, Australia.

His research interests include mechatronics, signal processing, control, measurement, and instrumentation.



Alireza Bab-Hadiashar (SM'04) received the B.Sc. degree in mechanical engineering from the University of Tehran, Tehran, Iran, in 1988, the MES degree in mechanical and mechatronics engineering from The University of Sydney, Sydney, Australia, in 1993, and the Ph.D. degree in computer vision from Monash University, Clayton, Australia, in 1997.

He is currently a Professor with the School of Aerospace, Mechanical and Manufacturing Engineering, RMIT University, Melbourne, Australia. He has made significant contributions to the establishment of mechatronics engineering degree programs in both Australia and Malaysia and has published numerous highly cited papers on optical flow, robust segmentation, and model selection techniques. His main research interests include development of robust estimation and segmentation techniques for computer vision applications and intelligent and robust sensory systems for new generation vehicle technologies.



Zhenwei Cao received the B.S. and M.E. degrees from Southeast University, Nanjing, China, in 1985 and 1988, respectively, and the Ph.D. degree from the University of Newcastle, Newcastle, Australia, in 2001, all in electrical engineering.

She is currently a Senior Lecturer with the Faculty of Engineering and Industrial Sciences, Swinburne University of Technology, Hawthorn, Australia. Her current research interests include robotics, mechatronics, control, and automation.



Ajay Kapoor received the B.Tech. and M.Tech. degrees from Banaras Hindu University, Varanasi, India, and the Ph.D. degree from the University of Cambridge, Cambridge, U.K.

He has over 25 years of experience in academia. He held a Professorship at Newcastle University, Newcastle upon Tyne, U.K., and was the Deputy Director of the Newcastle-based rail research center NEWRAIL. He is currently the Pro Vice Chancellor (International Research Engagement) and Deputy Dean of the Faculty of Engineering and Industrial Sciences, Swinburne University, Hawthorn, Australia. Since 2007, at Swinburne University, he has run the offices of the Associate Dean International and then Associate Dean Research. He also served as Higher Education representative to the University Council. He is the author of one book, several patents, and over 200 papers, articles, and reports, including four prize winning publications.

Dr. Kapoor is a member of several prestigious journal editorial boards. He was the Chair of the Executive Committee and the Treasurer of the U.K. and Ireland Section of the American Society of Mechanical Engineers.